ISSN 1063-7834, Physics of the Solid State, 2020, Vol. 62, No. 3, pp. 480–484. © Pleiades Publishing, Ltd., 2020.
Russian Text © The Author(s), 2020, published in Fizika Tverdogo Tela, 2020, Vol. 62, No. 3, pp. 422–426.

FERROELECTRICITY

Creation and Investigation of Metal—Dielectric–Semiconductor Structures Based on Ferroelectric Films

M. S. Afanas'ev[a], D. A. Kiselev[a, b], S. A. Levashov[a], A. A. Sivov[a], and G. V. Chucheva[a, *]

[a] *Kotelnikov Institute of Radioengineering and Electronics, Fryazino Branch, Russian Academy of Sciences, Fryazino, Russia*

[b] *National University of Science and Technology MISIS, Moscow, Russia*

** e-mail: gvc@ms.ire.mssi.ru*

Received October 18, 2019; revised October 18, 2019; accepted October 23, 2019

Abstract—The effect of the synthesis temperature on the microstructure and the electrophysical properties of metal–dielectric–semiconductor structures based on ferroelectric films of the composition $Ba_{0.8}Sr_{0.2}TiO_3$ upon the formation of *p*-type silicon substrates with [100] orientation is studied. It was experimentally established that an increase in the synthesis temperature leads to an improvement in the dielectric and piezoelectric properties of ferroelectric films. The temperature stability and stability in the behavior of the capacitance–voltage characteristics of MIS structures on the number of switching cycles are shown.

Keywords: metal–dielectric–semiconductor structures, ferroelectric films of the composition $Ba_{0.8}Sr_{0.2}TiO_3$, microstructure, scanning probe microscopy, capacitance–voltage characteristics, capacitance, switching cycles

DOI: 10.1134/S1063783420030026

1. INTRODUCTION

Recently, the prospects of creating a new generation of information processing and storage devices based on metal–dielectric–semiconductor (MIS) structures have been associated with the use of new structural materials both in composition and in structure. Ferroelectric materials are of great interest as structural materials in MIS structures for nonvolatile memory devices [1].

The solid solutions of barium–strontium titanate ($Ba_{1-x}Sr_xTiO_3$) are a promising composition of ferroelectrics for use in nonvolatile memory devices. The composition of $Ba_{1-x}Sr_xTiO_3$ has ferroelectric properties at room temperature. The dielectric constant of thin $Ba_{1-x}Sr_xTiO_3$ films remains almost unchanged over a wide temperature range [2].

In this paper the effect of the synthesis temperature on the microstructure and electrophysical properties of MIS structures based on $Ba_{0.8}Sr_{0.2}TiO_3$ films formed on *p*-type silicon substrates is studied.

2. MATERIALS AND METHODS OF THE EXPERIMENT

For studies, MIS structures were made, which are a *p*-type silicon substrate with an orientation of [100] and a thickness of 300 ± 10 μm, a ferroelectric film of the composition $Ba_{0.8}Sr_{0.2}TiO_3$ (BST), and an upper electrode made of nickel. A ferroelectric film with a thickness of 350 ± 25 nm was deposited on a silicon substrate by high-frequency sputtering at the Plasma-50SE installation (Russia). The design of the installation and the technique of film deposition are given in [3, 4]. The temperature of the substrate during the synthesis was 560°C (BST_{560}) and 620°C (BST_{620}). The upper nickel electrode was deposited onto the ferroelectric film by the electron beam method through a shadow mask on an A700QE/DI12000 installation (Germany). To improve nickel adhesion to the ferroelectric film, the structure was heated to 100 ± 5°C during deposition. Nickel deposition rate 2.0 ± 0.1 Å/s. The area of the nickel electrodes was 2.7×10^{-4} cm^2, and the thickness was 0.1 μm.

An X-ray diffraction study showed that for all samples a parallel arrangement of the axes of the film and the substrate was observed in the conjugation plane ([100] BST ‖ [100] *p*-Si).

The topography of the BST films was obtained in the contact mode using a MFP-3D SA scanning probe microscope (Asylum Research, USA) using a CSG10 cantilever (NT-MDT, Russia). The processes of local repolarization and residual piezoelectric hysteresis loops were obtained using piezoelectric response force microscopy (MFP) using an Asyelec-02 cantilever (Asylum Research, USA). Image processing and analysis implemented in the program Gwyddion.

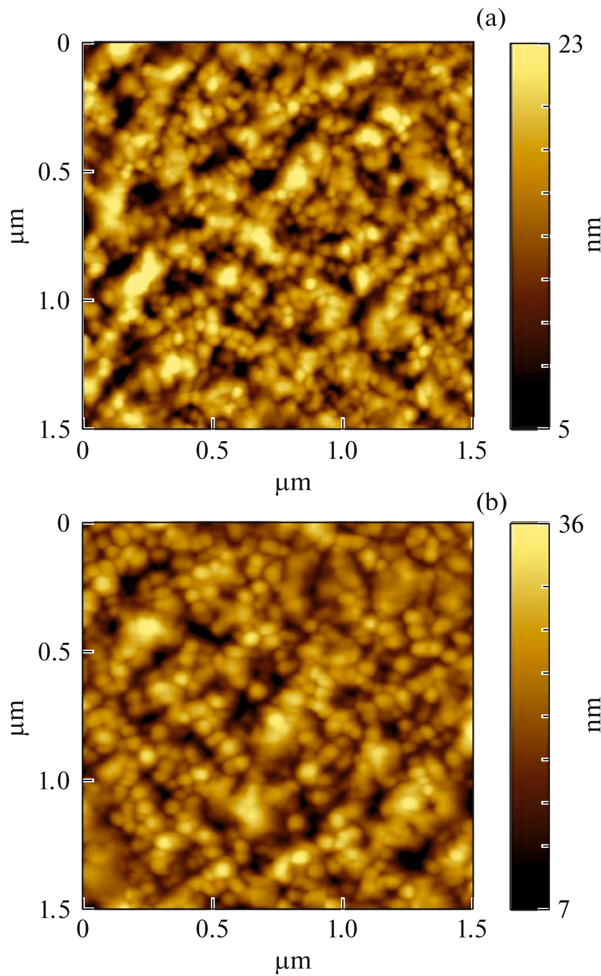

Fig. 1. Images of the surface of the films: (a) BST_{560} and (b) BST_{620}.

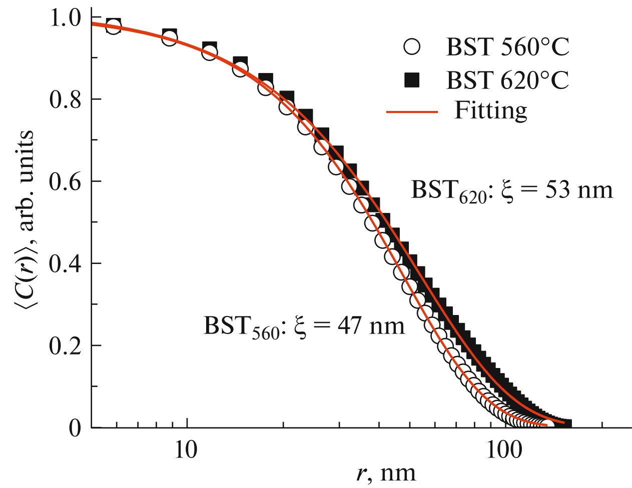

Fig. 2. Autocorrelation function profiles (symbols) and their approximation (lines) for the studied BST films.

Studies of the electrophysical properties of the obtained MIS structures were carried out on an automated measuring bench [5] using a precision Agilent E4980A LCR meter, a laptop computer with modified software, and a special camera equipped with a heat-stabilizing table. The effective permittivity of MIS structures is determined on the basis of measurements carried out by the method described in [6, 7].

3. RESULTS AND DISCUSSION

3.1. Scanning Probe Microscopy

In Fig. 1, the topography images of BST films synthesized at temperatures of 560 and 620°C are presented. It can be seen from the obtained topographic images that the films are formed from crystallites (grains). The root mean square surface roughness (*Rms*) was 3.8 and 4.3 nm for the BST_{560} and BST_{620}, respectively. To quantify the grain size (correlation length ξ), we used the autocorrelation function method described in detail in [8]. Figure 2 shows the result of approximating the correlation function to determine the average grain size in ferroelectric films. Calculations showed that for BST_{560} the average grain size was 47 nm, and for BST_{620} $\xi = 53$ nm.

In the investigated MIS structures, local polarization switching is observed under the action of a constant voltage. In Fig. 3a, the induced piezoelectric response signal for a BST_{560} film is presented as an example of the effect of repolarization. The induced macrodomain regions were created by scanning the film with a constant voltage applied to a conductive cantilever, which played the role of the upper electrode. Thus, two polarized regions with an area of 8×8 μm (“bright region”—polarization at +25 V) and 4×4 μm (“dark region”—polarization at –25 V) were created by the potential. The resulting induced domains are stable for several hours of continuous scanning.

Using the polarization switching spectroscopy module in the MFP mode, it becomes possible to obtain the residual piezoelectric hysteresis loops (Fig. 3b) and thereby study the effect of local polarization switching at the nanoscale. It was experimentally established that the BST_{620} film is characterized by higher values of the piezoelectric coefficient ($d_{33} \approx$ 147 pm/V at +20 V) compared to BST_{560}. The value of the effective piezoelectric coefficient obtained by us agrees with the theoretical work [9], in which the nonlinear thermodynamic model was used to calculate the piezoelectric coefficient in BST epitaxial films depending on the composition (Ba/Sr), misfit strains, and temperature.

In addition, for the films under study, the piezoelectric hysteresis loops have an asymmetric shape, which may be due to the presence of a built-in electric field or to the internal bias field caused by oxygen vacancies and space charge in the case of horizontal

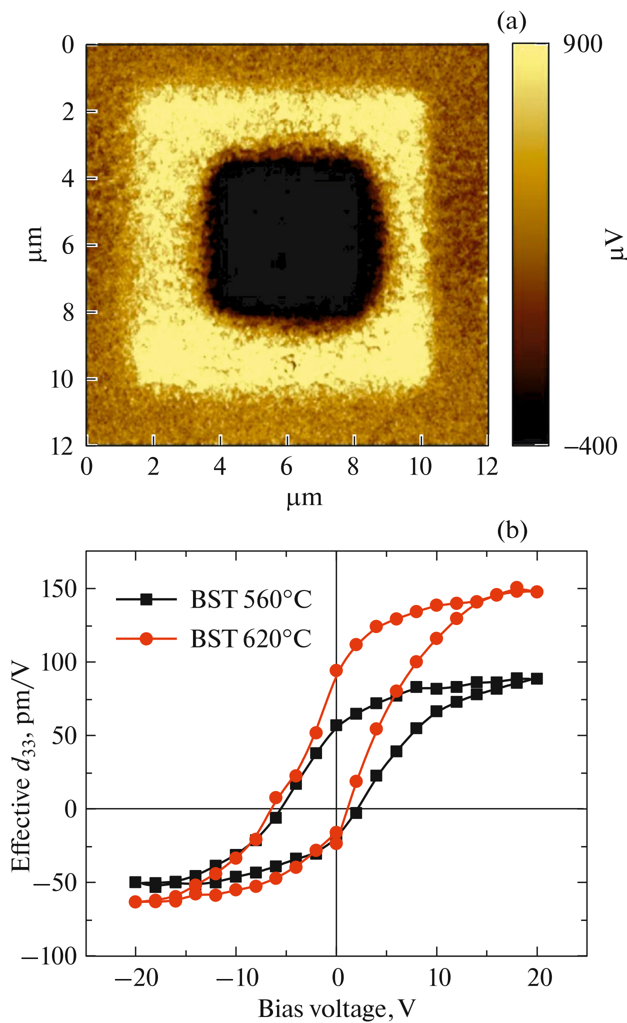

Fig. 3. Signal of the induced piezoelectric response of the BST_{560} film (a), the residual piezoelectric hysteresis loops for the studied films (b).

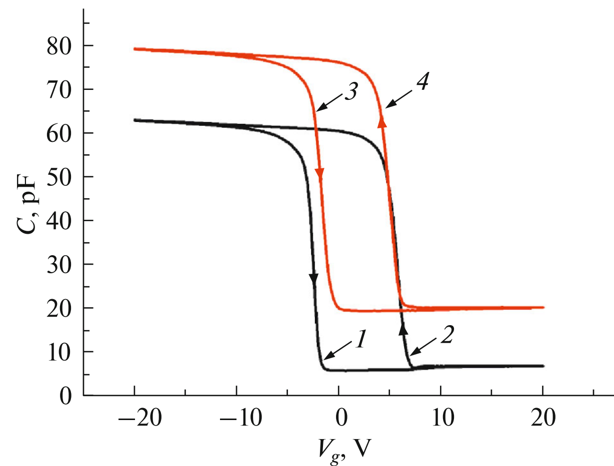

Fig. 4. Capacitance–voltage characteristics of the MIS structures BST_{560} (curves *1*, *2*) and BST_{620} (curves *3*, *4*), measured at room temperature at a frequency of 100 kHz.

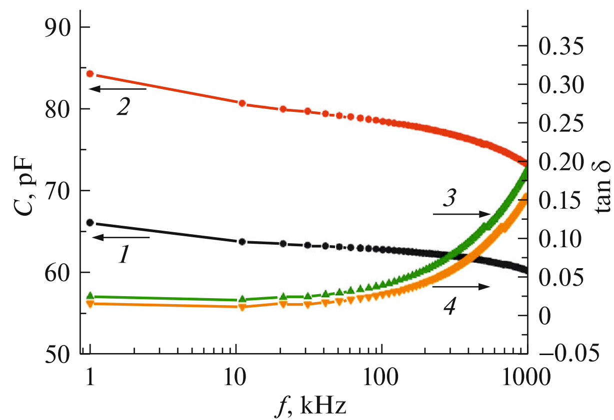

Fig. 5. Frequency dependences of the capacitance and dielectric loss tangent of the MIS structures BST_{560} (curves *1*, *3*) and BST_{620} (curves *2*, *4*), measured at a constant bias voltage $V_g = -20$ V.

bias of the hysteresis loop [10]. The vertical displacement is due to different materials of the cantilever (Ti/Ir) and the lower electrode (Si), which affects the contact potential difference between them [11].

2.2. Electrophysical properties

In Fig. 4, the capacitance–voltage characteristics (CVC) of the MIS structures BST_{620} and BST_{560}, measured at room temperature at a frequency of 100 kHz are presented. A bias voltage V_g from −20 to +20 V (curves *1*, *3*) and vice versa (curves *2*, *4*) was applied to the sample with a step of 0.25 V and a measurement signal amplitude of 25 mV with a data reading speed of 3 points per second.

The dependences of the capacitance on the bias voltage are in the form of a loop (hysteresis). The loop width for both MIS structures is 7 ± 0.2 V. The vertical axis of symmetry of the loop of structures is shifted toward $V_g \simeq +2.6$ V. The shift of the loop relative to the point $V_g = 0$ V could be due to the presence of an internal electric field in the ferroelectric film, the appearance of which is due to differences in the structure and charge state of the Si/BST interface.

In the structure of BST_{620}, the CVC loop has a more symmetrical shape (see Fig. 4, curves *3*, *4*) than in the structure of BST_{560} (see Fig. 4, curves *1*, *2*). This suggests a more stable behavior of the BST_{620} structure.

The structures of the BST_{620} are characterized by higher capacitance values compared to similar structures of the BST_{560}. The maximum capacitance values were observed at $V_g \approx -20$ V and amounted to 63 pF and 78 pF for BST_{560} and BST_{620}, respectively.

In Fig. 5, the frequency dependences of the capacitance and dielectric loss tangent of the MIS structures

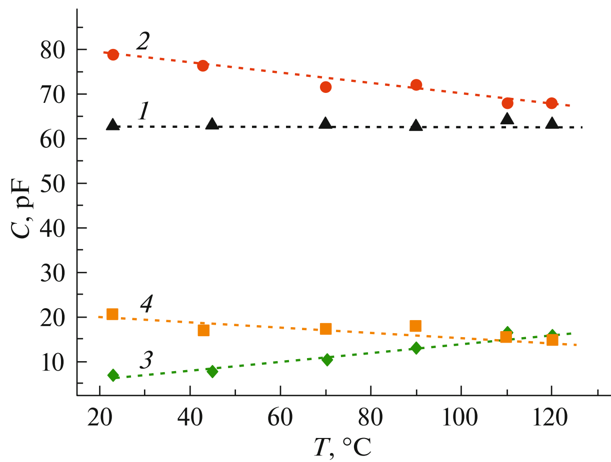

Fig. 6. Temperature dependences of the capacitance of the MIS structures BST_{560} (curves *1*, *3*) and BST_{620} (curves *2*, *4*).

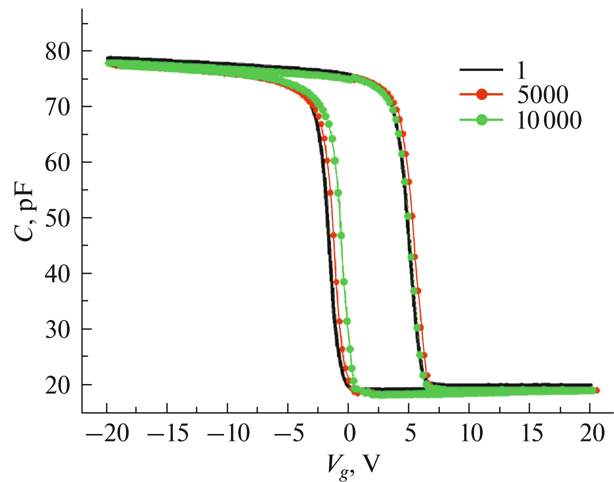

Fig. 7. Capacitance–voltage characteristics of the BST_{620} structure depending on switching cycles.

BST_{620} and BST_{560} measured at room temperature and a constant bias voltage $V_g = -20.0$ V are presented. In both samples, capacitances decrease with increasing frequency. In this case, the structure of BST_{620} (curve *2*) demonstrates higher capacitance values in the range 1–1000 kHz than the structure of BST_{560} (curve *1*).

The graph of the frequency dependence of the dielectric loss tangent for both objects is identical and has the form of a straight line parallel to the abscissa axis in the range 1–70 kHz, turning into a sharp increase in the range 70–1000 kHz. The value of the dielectric loss tangent on average for both curves is 0.02 in the frequency range 1–70 kHz and increases to 0.17 in the range 70–1000 kHz.

In Fig. 6, the temperature dependences of the sample capacitance at $V_g = 20$ V (curves *1*, *2*) and $V_g = -20$ V (curves *3* and *4*) are presented from the temperature dependences of the CVC of the MIS structures. The CVC of the objects were measured in the voltage range from –20 to + 20 V in the temperature range from 23 to 120°C at a frequency of 100 kHz.

With increasing temperature, a slight decrease in the capacitance is observed for the BST_{620} structure at $V_g = -20$ V. On the contrary, the capacitance of the BST_{560} structure does not change at $V_g = -20$ V and increases insignificantly at $V_g = +20$ V. This circumstance allows us to conclude that the structure of the BST_{560} is more thermostable compared to the structure of the BST_{620}.

In Fig. 7, the CVC of the BST_{620} structure in depending on switching cycles are presented. A voltage of 5 V with an interval of 0.1 s was applied to the sample for 0.1 s. 10 000 cycles (on/off) were conducted. The CVC were measured after 5000 and 10 000 switching cycles.

It was found that after 5000 cycles of switching the structure of the BST_{620}, the capacitance value and the shape of the curve do not change. After 10 000 switching cycles, the capacitance value also does not change, but a slight narrowing of the loop by 0.3 V to the right is observed.

CONCLUSIONS

The investigations indicated the influence of the synthesis temperature of thin BST films on the dielectric characteristics of MIS structures based on them. It was established that the samples synthesized at a temperature of 620°C have higher capacitance values (and, correspondingly, permittivity) in comparison with structures obtained at 560°C.

The results obtained by the MFP method are consistent with dielectric measurements: with increasing synthesis temperature, both the dielectric and piezoelectric characteristics of BST 80/20 films increase.

It was found that the CVC of the BST_{620} structure after 5000 switching cycles remain unchanged.

FUNDING

This work was carried out as part of a state assignment and was partially supported by the Russian Foundation for Basic Research (projects nos. 18-29-11029, 19-07-00271 and 19-29-03042). Investigations by methods of scanning probe microscopy were performed on the equipment of the Central Scientific and Practical Center "Materials Science and Metallurgy" of the National University of Science and Technology "MISIS."

CONFLICT OF INTEREST

The authors declare that they have no conflicts of interest.

REFERENCES

1. K. A. Vorotilov, V. M. Mukhortov, and A. S. Sigov, *Integrated Ferroelectric Devices*, Ed. by A. S. Sigov (Energoatomizdat, Moscow, 2011) [in Russian].
2. V. M. Mukhortov and Yu. I. Yuzyuk, *Heterostructures Based on Nanoscale Ferroelectric Films: Production, Properties and Application* (YuNTs RAN, Rostov-on-Don, 2008) [in Russian].
3. M. S. Ivanov and M. S. Afanas'ev, Phys. Solid State **51**, 1328 (2009).
4. D. A. Kiselev, M. S. Afanasiev, S. A. Levashov, and G. V. Chucheva, Phys. Solid State **57**, 1151 (2015).
5. E. I. Gol'dman, A. G. Zhdan, and G. V. Chucheva, Instrum. Exp. Tech. **40**, 841 (1997).
6. T. Hamano, D. J. Towner, and B. W. Wessels, Appl. Phys. Lett. **83**, 5274 (2003).
7. P. M. Suherman, T. J. Jackson, Y. Y. Tse, I. P. Jones, R. I. Chakalova, M. J. Lancaster, and A. Porch, J. Appl. Phys. **99**, 104101 (2006).
8. M. S. Afanasiev, D. A. Kiselev, S. A. Levashov, A. A. Sivov, and G. V. Chucheva, Phys. Solid State **61**, 1910 (2019).
9. H. Khassaf, N. Khakpash, F. Sun, N. M. Sbrockey, G. S. Tompa, T. S. Kalkur, and S. P. Alpay, Appl. Phys. Lett. **104**, 202902 (2014).
10. Q. Lin, D. Y. Wang, Z. G. Chen, W. F. Liu, and S. Li, ACS Appl. Mater. Interfaces **7**, 26301 (2015).
11. P. Maksymovych, N. Balke, S. Jesse, M. Huijben, R. Ramesh, A. P. Baddorf, and S. V. Kalinin, J. Mater. Sci. **44**, 5095 (2009).

Translated by N. Petrov